G. Zhou, Y. Ye, W. Zuo, X. Zhou, X.Xu. 2018. "Fast and efficient prediction of finned-tube heat exchanger performance using wet-dry transformation method with nominal data". Applied Thermal Engineering. 145, pp. 133-146, DOI: 10.1016/j.applthermaleng.2018.09.020.

Fast and efficient prediction of finned-tube heat exchanger performance using wet-dry transformation method with nominal data

G. Zhou[1,2] Y. Ye[3] W. Zuo[3*] X. Zhou[1] X. Wu[4]

[1] Academy of Building Energy Efficiency, Guangzhou University, Guangzhou, Guangdong 510006, China
[2] Tianhe College of Guangdong Polytechnic Normal University, Guangzhou, Guangdong 510540, China
[3] Department of Civil, Environmental and Architectural Engineering, University of Colorado Boulder, Boulder, CO 80309, USA
[4] Nanjing TICA Climate Solutions Co., LTD, Nanjing, Jiangsu 210046, China

[*]Corresponding author. E-mail address: Wangda.Zuo@Colorado.EDU

Abstract

Water-to-air finned-tube heat exchanger (FTHE) is a common component in air-conditioning systems. Mathematical models of water-to-air FTHE under the wet-cooling condition are necessary in evaluating the performance of air-conditioning system with water-to-air FTHEs during the system design phase. However, existing water-to-air FTHE models are computationally expensive and require detailed geometric data, which hinder the model applications during the system design phase. To address the above limitations, the current paper proposes a new water-to-air FTHE model which is computationally efficient, relatively accurate and only requires nominal data as inputs. The new water-to-air FTHE model is derived using wet-dry transformation method and the heat transfer process is calculated using the nominal data. Then the model is implemented in Modelica, which is an equation-based, object-oriented modeling language. In addition, experimental measurements of a water-to-air FTHE are conducted. The new model is then evaluated by experimental data and an existing model. The results show that the relative deviations of outlet temperatures and heat transfer rate between the modeled and experimental data are within 7% and 11%, respectively, which is much better than the existing model (19% and 13%). In addition, the new model is 1,047 times faster than the existing model.

Key words: finned-tube heat exchanger, model, wet-dry transformation method, Modelica

Nomenclature

A	heat transfer area, m^2
B	local atmospheric pressure, Pa
b	coefficient from the boundary layer analysis
c_p	specific heat capacity under constant pressure, $\mathrm{J/(kgK)}$
$\dot{C}$	heat capacity rate, $\mathrm{J/(Ks)}$
c	constant
d	humidity ratio, $\mathrm{kg/kg_{da}}$ or differential symbol
H	specific enthalpy, $\mathrm{J/kg_{da}}$
h	sensible convective heat transfer coefficient, $\mathrm{W/(m^2K)}$
h_m	convective mass transfer coefficient, $\mathrm{kg/(m^2s)}$
Le_f	Lewis factor, dimensionless
Le	Lewis number
$\dot{m}$	mass flow rate, $\mathrm{kg/s}$
N	number of pipe segments in WCCF model
n	exponent of heat transfer correlation
NTU	number of heat transfer units, dimensionless
Nu	Nusselt number, dimensionless
$\dot{Q}$	(total) heat transfer rate, W
Re	Reynolds number, dimensionless
T	temperature, K
X	water vapor mass fraction, dimensionless
U	overall heat transfer coefficient, $\mathrm{W/(m^2K)}$

Greek letters

ε	heat transfer effectiveness, dimensionless
ζ	contact factor, dimensionless
η	fin efficiency, dimensionless
χ	factor for thermal variation of fluid properties

Subscripts

0	nominal condition
3	saturation state point of tube surface
a	air side of heat exchanger
in	inlet
max	maximum
min	minimum
out	outlet
s	sensible heat or saturation state
t	overall
v	condensed water vapor
w	water side of heat exchanger

RH	relative humidity, dimensionless	i	mark number of the microelements
r	ratio of convective heat transfer coefficients, dimensionless		

1. Introduction

As a common component in air handling units, water-to-air finned-tube heat exchangers (FTHEs) are widely used for various air-conditioning systems to control air temperature and humidity [1]. The water-to-air FTHE consists of a set of parallel round tubes which are distributed uniformly in a block with parallel fins. Water flows inside the tubes and indirectly interacts with the air passing over the tubes. Air dehumidification occurs if the surface temperature of the heat exchanger is lower than the air dew point temperature. As a result, there are simultaneous heat and mass transfers on the external surface of tubes and fins [2]. This condition is called "wet-cooling process" [3-5]. A model of water-to-air FTHE with wet-cooling condition is usually necessary to evaluate performances and conduct optimizations. In order to achieve wide engineering applications, it is of great importance to develop an accurate and computationally efficient water-to-air FTHE model [6]. In addition, the model utilized in design phase should be independent of operational data, only with input data which are available during the design phase [7].

The existing water-to-air FTHE models under the wet-cooling condition can be classified into three catagories [8, 9]: Numerical models [10-18], Analytical models [5, 19-22] and lumped models [23-35]. The numerical models discretize the space of cooling coil into numerous elements and the results of each element are obtained by using iterative algorithms [10-14]. These models can be used to systematically and comprehensively analyze the heat transfer process and provide accurate and informative results for optimal design of the heat exchanger. However, those models are computationally expensive [5, 8, 26, 36]. In some cases, numerical models have problems related to convergence, stiffness and stability [21, 33]. Moreover, most of models require details of geometric data (e.g. length and diameter of tubes, thickness of the fins), which are difficult to obtain during the design phase.

The analytical models solve differential equations for the heat and mass transfer process in FTHE using advanced algorithms, such as Fourier transformations [37], Laplace transformations [19, 20, 22], matrix operations [38], and integral methods with simplification [5, 21]. Although analytical models have high computational efficiency, some transform methods (e.g. Laplace transformations) need to inverse the solution from the s-domain to the time domain, but the inversation may fail in some cases[21, 33]. In addition, the analytical models still require the details of geometric data, which hinders its engineering appliations.

The lumped models utilize the enthalpy difference between air and coolant to simulate the heat and mass transfer process [23-35]. The lumped models are relatively accurate and computationally efficient [5, 8, 26]. However, the existing lumped models still require geometric data, specific heat transfer coefficients, and some operational data, which are difficult to obtain during the design phase.

To improve the existing models for the water-to-air FTHE with wet-cooling conditions, current research proposes a new model with two innovations: 1) It adopts a wet-dry transformation method (WDTM) [27] so that a classic effectiveness-NTU method [25] can be applied in these equivalent dry-cooling processes of the wet-cooling conditions. As a result, the new model is faster than the numerical models and simpler than the analytical models; 2) The new model calculates the heat transfer using nominal data available in the design phase and does not require geometric data, specific heat transfer coefficients, and operational data. These characteristics of the new model will facilitate the optimal design of the air-conditioning system in the design phase.

In the current paper, section 2 illustrates derivation of the new proposed water-to-air FTHE model and determinations of model parameters. Section 3 shows the implementation in Modelica. Then, experimental measurement is shown in section 4. Finally, the new model is evaluated by experimental data and an existing model in section 5.

2. Mathematical Description

The newly proposed water-to-air FTHE model is based on the wet-dry transformation method [27], utilizing a hypothetical equivalent dry-cooling condition to reflect the water-to-air FTHEs performance in the presence of wet-cooling condition. Then the classic effectiveness-NTU method [25] is applied in this equivalent dry-cooling process to calculate heat tranfer under wet-cooling condition. To simplify the model, several assumptions are adopted as follows: 1) The fouling and thermal resistances of different materials are neglected; 2) There is no water leakage or heat loss; 3) The air pressure is 1 bar; 4) The specific heat capacity and the overall fin efficiency are constant values; 5) The model is applied in steady state. The following description of the new FTHE model summaries the main steps of mathematical derivation and the relevant detailes are provided in Appendix A.

2.1. Equivalent Dry-cooling Condition

Compared with a wet-cooling condition, the equivalent dry-cooling condition has the same mass flow rate (air/water), contact factor, inlet and outlet air enthalpies or water temperature [27]. The contact factor ζ reflects the close extent of the final air state to its saturation state. According to the above definitions, the heat transfer rates of the wet-cooling condition and its equivalent dry-cooling condition are identical.

Fig. 1 shows the wet-cooling process and its equivalent dry-cooling process on the air side [27]. Line "1-2" represents a wet-cooling process with moist air flowing through a FTHE. Line "1′-2′" is the equivalent dry-cooling condition of process "1-2". Line "1-1′" and "2-2′" are two constant enthalpy lines. Point 1 and point 2 represent the inlet and outlet states in the wet-cooling process respectively. Similarly, point 1′ and point 2′ are the inlet and outlet states of the equivalent dry-cooling condition. Point 3 and point 3′ are the saturation states on the tube surface under the wet-cooling condition and its equivalent dry-cooling condition, respectively. Point 3 and point 3′ are overlapped in the psychrometric chart.

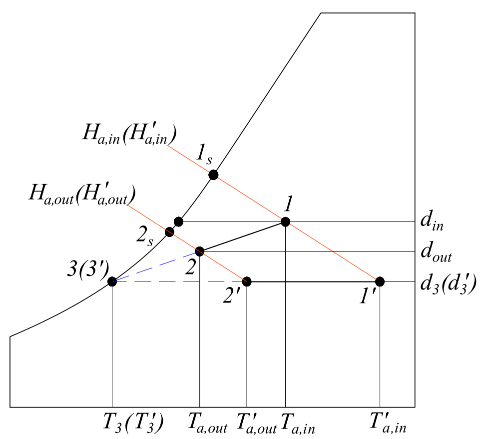

Fig. 1. Wet-cooling condition and its equivalent dry-cooling condition in the psychrometric chart

The relationship between the wet-cooling condition and its equivalent dry-cooling condition can be expressed as [27]:

$$\zeta = \frac{H_{a,in} - H_{a,out}}{H_{a,in} - H_3} = \frac{H'_{a,in} - H'_{a,out}}{H'_{a,in} - H_3}, \tag{1}$$

and

$$\zeta = \frac{T_{a,in} - T_{a,out}}{T_{a,in} - T_3} = \frac{T'_{a,in} - T'_{a,out}}{T'_{a,in} - T_3}. \tag{2}$$

where H is specific enthalpy of the air; T is temperature of medium; ζ is the contact factor. The variables with superscript "$'$" are the equivalent dry-cooling condition; the variables with subscript "a" are on the air side; the variables with subscript "in" and "out" are the ones of the inlet and outlet of the heat exchanger, respectively.

The outlet states of the FTHE under wet-cooling condition $H_{a,out}$ and $T_{a,out}$ can be obtained using the Eq. (1) and Eq. (2):

$$H_{a,out} = H_{a,in} - \frac{T'_{a,in} - T'_{a,out}}{T'_{a,in} - T_3}(H_{a,in} - H_3), \tag{3}$$

and

$$T_{a,out} = T_{a,in} - \frac{T'_{a,in} - T'_{a,out}}{T'_{a,in} - T_3}(T_{a,in} - T_3). \tag{4}$$

The values of $H_{a,out}$ and $T_{a,out}$ can be obtained if $T'_{a,in}$, $T'_{a,out}$, H_3 and T_3 are known. The key in calculation of $T'_{a,in}$, $T'_{a,out}$, H_3 and T_3 is the convective heat transfer coefficients on air/water sides of the heat exchanger with the equivalent dry-cooling condition. Thus, section 2.2 will describe the procedure to calculate the convection heat transfer coefficients. Then section 2.3 will show the calculation of $T'_{a,in}$, $T'_{a,out}$, H_3 and T_3.

2.2. Calculation of Convective Heat Transfer Coefficients

In the wet-cooling process, heat transfer at the air side of the water-to-air FTHE is driven by the enthalpy difference between main stream and saturated air near the tube surface. The equation can be written as [39]:

$$d\dot{Q} = \frac{\eta_t h_a (H - H_3) dA}{c_{p,a} Le_f}, \tag{5}$$

where dA is a discretized heat transfer area; $d\dot{Q}$ is the heat transfer rate in dA; η_t is overall fin efficiency [25]; h_a is sensible convective heat transfer coefficient; $c_{p,a}$ is the specific heat capacity of the air; Le_f is Lewis factor that reflects the relative strength of heat transfer and mass transfer [40]. Le_f is a parameter given by users in this new model. The selection of Le_f is discussed in section 2.4.2. Based on Eqs. (1), (2) and (5), the contact factor ζ can be derived as (details see Appendix A.1):

$$\zeta = 1 - exp\left[-\frac{(\eta_t hA)_a}{\dot{C}_a\, Le_f}\right] = 1 - exp\left[-\frac{(\eta_t hA)'_a}{\dot{C}_a}\right], \tag{6}$$

where A is the total heat transfer area; $\dot{C}_a$ is the heat capacity rate of air flow, and $\dot{C} = \dot{m}c_p$. From Eq. (6), we can obtain the relationship between convective heat transfer coefficients in wet-cooling condition and equivalent dry-cooling condition on the air side:

$$(\eta_t hA)'_a = (\eta_t hA)_a\, {Le_f}^{-1}. \tag{7}$$

In Eq. (7), Le_f is defined as a parameter in this new model. If the $(\eta_t hA)_a$ is known, the heat conductivity $(\eta_t hA)'_a$ under its equivalent dry-cooling condition can be obtained. Then based on Eq. (6), the value of ζ can be calculated.

For the water side, the wet-cooling process and its equivalent dry-cooling process are the same. As a result, the relationship between convective heat transfer coefficients in the wet-cooling condition and its equivalent dry-cooling condition at the water side is:

$$(hA)'_w = (hA)_w. \tag{8}$$

where, w means water side; h_w and h'_w are the convective heat transfer coefficients of the wet-cooling condition and its equivalent dry-cooling condition on the water side respectively.

The next step is solving $(\eta_t hA)_a$ and $(hA)_w$ in the actual conditions. For the air side, the h_a is correlated with $h_{a,0}$ [14]:

$$(\eta_t hA)_a = \chi_a\left(T_{a,in}\right)(\frac{\dot{m}_a}{\dot{m}_{a,0}})^{n_a}(\eta_t hA)_{a,0}, \tag{9}$$

where $h_{a,0}$ is the convective heat transfer coefficient at the air side under the nominal condition; n_a is the exponent of Reynolds number in the convective heat transfer correlation on the air side. In this new FTHE model, n_a is a parameter, which needs to be given in advance. The selection of n_a is discussed in section 2.4.3. The $\chi_a(T_{a,in})$ illustrates the variations of air properties, which could be regarded as a function of the inlet air temperature, i.e.[14]:

$$\chi_a\left(T_{a,in}\right) = 1 + 7.8532 \times 10^{-4}(\,T_{a,in} - T_{a,in,0}). \tag{10}$$

If the nominal $(\eta_t hA)_{a,0}$ is known, the $(\eta_t hA)_a$ can be calculated based on Eq. (9) and Eq. (10).

For the water side, the h_w has the following correlation with $h_{w,0}$ [14]:

$$(hA)_w = \chi_w\left(T_{w,in}\right)(\frac{\dot{m}_w}{\dot{m}_{w,0}})^{n_w}(hA)_{w,0}, \tag{11}$$

where, $h_{w,0}$ is the convective heat transfer coefficient at the water side under the nominal condition; n_w is the exponent of water flow velocity in the convective heat transfer correlation on the water side; $\chi_w\left(T_{w,in}\right)$ is the variable defining the physical properties of water. In this new FTHE model, n_w is a parameter and needs to be given by users. The selection of n_w is discussed in section 2.4.3. The $\chi_w\left(T_{w,in}\right)$ is calculated as follows [14]:

$$\chi_w\left(T_{w,in}\right) = 1 + \frac{0.014}{1 + 0.014(T_{w,in,0} - 273.15)}\left(T_{w,in} - T_{w.in,0}\right). \tag{12}$$

If the nominal $(\eta_t hA)_{w,0}$ is known, the $(\eta_t hA)_w$ can be calculated based on Eq. (11) and Eq. (12).

The next task is to calculate $(\eta_t hA)_{a,0}$ and $(hA)_{w,0}$ under nominal condition. The nominal $(\eta_t hA)_{a,0}$ can be derived by [7]:

$$(\eta_t hA)_{a,0} = (UA)_0(r + 1), \tag{13}$$

where, U is overall heat transfer coefficient; r is the quotient of the convective heat transfer coefficients on the two sides (water/air) of the heat exchanger under nominal condition, i.e.,

$$r = \frac{(\eta_t hA)_{\mathrm{a,0}}}{(hA)_{\mathrm{w,0}}}. \tag{14}$$

where r is set as a parameter in this new FTHE model. The selection of r is discussed in section 2.4.2.

In the water-to-air FTHEs, the mass transfer has trivial impacts on the sensible heat transfer [39]. Thus, the mass transfer and the sensible heat transfer could be assumed to be independent. In the nominal situation, the sensible heat flow rate is $\dot{Q}_{s,0}$, the overall heat transfer coefficient is U_0 , inlet temperatures and mass flow rates at air/water sides are $\dot{m}_{a,0}$, $\dot{m}_{w,0}$, $T_{a,in,0}$ and $T_{w,in,0}$, respectively. Then, the effectiveness-NTU method is used to calculate $(UA)_0$ (see details in Apendix A.2). In the new FTHE model, the nominal data ($\dot{Q}_{s,0}$, $\dot{m}_{a,0}$, $\dot{m}_{w,0}$, $T_{a,in,0}$, $T_{w,in,0}$ and $flow\ arrangement$) are set as nominal parameters. The $flow\ arrangement$ is associated with the structure of heat exchanger, such as flow arrangement, cross flow arrangement, etc (see details in Apendix A.2). The selections of these parameters are discussed in section 2.4.1.

After obtaining the convective heat transfer coefficients $(\eta_t hA)'_a$ and $(hA)'_w$ under the equivalent dry-cooling condition, the next step is to simulate the heat transfer process in the equivalent dry-cooling process.

2.3. Heat Transfer Calculation

The heat transfer process under the equivalent dry-cooling condition is simulated by adopting the effectiveness-NTU method. The thermal resistance of the materials and the fouling on different surfaces are neglected [41]. Based on the effectiveness-NTU method, the heat transfer effectiveness ε' under the equivalent dry-cooling condition can be obtained. Based on the ε', $T'_{a,in}$ can be calculated by (see details in Apendix A.3):

$$T'_{a,in} = \frac{\dot{C}_{min}\,\varepsilon' T_{w,in} - \dot{C}_a \zeta T_3}{\dot{C}_{min}\varepsilon' - \dot{C}_a \zeta}, \tag{15}$$

where $\dot{C}_{min}$ is the minimum value of $\dot{C}_a$ and $\dot{C}_w$. Until now, only T_3 remains unknown. The quantitative relationship between saturation humidity ratio d_3 and saturation temperature T_3 is [42]:

$$d_3 = \frac{622}{7.5\mathrm{B} \cdot \exp\left[-18.5916 + \frac{3991.11}{(T_3 - 39.31)}\right] - 1}, \tag{16}$$

where B is local atmospheric pressure (101,325 Pa).

As Fig. 1 shown, the enthalpy, humidity ratio and temperature of point $1'$ are $H_{a,in}$, d_3 and $T'_{a,in}$, respectively. The relationship can be expressed as [43]:

$$H_{a,in} = 1006(T'_{a,in} - 273.15) + 1000 \times [2501 + 1.86(T'_{a,in} - 273.15)]d_3. \tag{17}$$

According to Eqs. (15), (16) and (17), $T'_{a,in}$, T_3 and d_3 can be obtained. H_3 is calculated by using the function of the enthalpy, humidity ratio and temperature as Eq. (17). The $T'_{a,out}$ can be obtained according to Eq. (2). Finally, $H_{a,out}$ and $T_{a,out}$ are calculated by Eq. (3) and Eq. (4).

2.4. Selection of Model Parameters

According to the mathematical description of the newly proposed FTHE model, there are some model parameters to be defined by the users: $\dot{Q}_{s,0}$, $\dot{m}_{a,0}$, $\dot{m}_{w,0}$, $T_{a,in,0}$, $T_{w,in,0}$, $flow\ arrangement$, r, $Le_{f,0}$, n_a and n_w. The detailed definitions of these parameters are described above and their selections are discussed below.

2.4.1. Selection of Nominal Parameters

The nominal condition is decided by users during the design phase. It can be the design condition or the maximum load condition. The nominal parameters ($\dot{m}_{a,0}$, $\dot{m}_{w,0}$, $T_{a,in,0}$ and $T_{w,in,0}$) are selected from the nominal data of the water-to-air FTHE, which are often available from the manufacturers. It is noticed that the heat transfer coefficients of this newly proposed model are derived from the nominal sensible heat transfer rate $\dot{Q}_{s,0}$ rather than the nominal total heat transfer rate $\dot{Q}_0$. The $\dot{Q}_{s,0}$ can be defined by users or calculated using

$$\dot{Q}_{s,0} = \dot{m}_{a,0}(T_{a,in,0} - T_{a,out,0}) \tag{18}$$

where $T_{a,out,0}$ is the outlet air temperature in the nominal condition.

The selection of $flow\ arrangement$ is determined by the configuration type of heat exchanger. There are six different flow arrangements of heat exchanger corresponding to six different equations for ε and NTU [29]. In other words, the selection of the parameter $flow\ arrangement$ is selecting equations for ε and NTU. When the number of the tube rows of an water-to-air FTHE is above three, it can be considered as the counter flow arrangement [39].

2.4.2. Selection of r and Le_f

There is an analytical formula for the calculation of r [7]:

$$r \approx \frac{a_2}{a_1}\left(\frac{V_{a,0}}{V_{w,0}}\right)^{0.8} \tag{19}$$

where $a_1 = 1.025$ and $a_2 = 0.208$, respectively. The $V_{a,0}$ is the face air velocity of the heat exchanger and $V_{w,0}$ is the water velocity in tube under nominal condition. In a cooling coil or tube, the face air velocity V_a is generally between 1.0 $\mathrm{m/s}$ and 3.0 $\mathrm{m/s}$, and V_w is between 1.0 $\mathrm{m/s}$ and 2.0 $\mathrm{m/s}$ [44]. Thus, according to Eq. (19), r is in the range from 0.1 to 0.5.

A Lewis factor correlation can be represented by numerically simulated results [45]:

$$Le_f = -1.331 + \frac{3.853}{RH} - \frac{2.231}{RH^2} + \frac{0.421}{RH^3} - \frac{26.21}{Re} \tag{20}$$

where, RH is the inlet relative humidity of the air and the range of RH ranges from 35% to 100%, Re is Reynolds number based on V_a. For Eq. (20), the range of V_a is between 0.30 $\mathrm{m/s}$ and 3.5 $\mathrm{m/s}$. Since V_a has minor impacts on the variation of Le_f [45], to simplify Eq. (20), we can ignore $26.21/Re$ in Eq. (20) and get $Le_f \in [0.712, 1.285]$ when $RH \in [0.35, 1]$. In addition, the literature indicates that the value of Lewis factor Le_f is roughly between 0.6 and 1.2 [46]. Considering these two analyses, we select $Le_f \in [0.6, 1.3]$. It is worth to mention that Lewis factor Le_f varies a lot under different operating conditions. To simplify this issue, the current paper adopts the nominal Lewis factor to represent the actual Lewis factor ($Le_f = Le_{f,0}$).

Once the nominal data are determined, only the parameters r, $Le_{f,0}$, n_a and n_w are unknown. Based on the Eq. (9) and Eq. (11), when conducting the heat transfer calculation using the new FTHE model under the nominal condition, it has nothing to do with n_a and n_w. Thus, we only need to determine r and $Le_{f,0}$ in this case. Under the nominal condition, r and $Le_{f,0}$ are the values that can minimize the relative deviation between the calculated and measured values of heat transfer rats:

$$\min\left(\sqrt{\left(\frac{\dot{Q}_0^c-\dot{Q}_0}{\max\left|\dot{Q}_0^c-\dot{Q}_0\right|}\right)^2+\left(\frac{\dot{Q}_{s,0}^c-\dot{Q}_{s,0}}{\max\left|\dot{Q}_{s,0}^c-\dot{Q}_{s,0}\right|}\right)^2}\right)=\min\left(f\left(r,\ Le_{f,0}\right)\right) \tag{21}$$

$s.t.$

$$0.1\leq r\leq 0.5,$$

$$0.6\leq\ Le_{f,0}\leq 1.3,$$

where $\dot{Q}_0^c$ and $\dot{Q}_{s,0}^c$ are the calculated values of total heat transfer rate and sensible heat transfer rate under the nominal condition.

2.4.3. Selection of n_a and n_w

This paper proposes to identify the heat transfer correlations related to the type of selected product from literatures and determine the value of n_a accordingly. The n_a is between 0 and 1 with a common range from 0.34 to 0.95 [7, 44, 47-54]. In the current paper, we select $n_a = 0.65$, which is approximately the median value of the range. For the n_w, 0.8 or 0.85 is commonly selected [39, 55]. In this work, we adopt $n_w = 0.85$.

3. Implementation

The new FTHE model is implemented using Modelica, an equation-based, object-oriented modeling language [56]. As an effective and promising modeling approach for building energy and control system, the Modelica has been widely used to conduct rapid prototyping of innovative building energy systems, model-based building control, and simulation of zero energy communities [57-64]. Our implementation is based on the free open-source Modelica Buildings Library [14, 65]. The following part introduces the detailed implementation of the newly proposed FTHE model.

3.1. Numerical Scheme

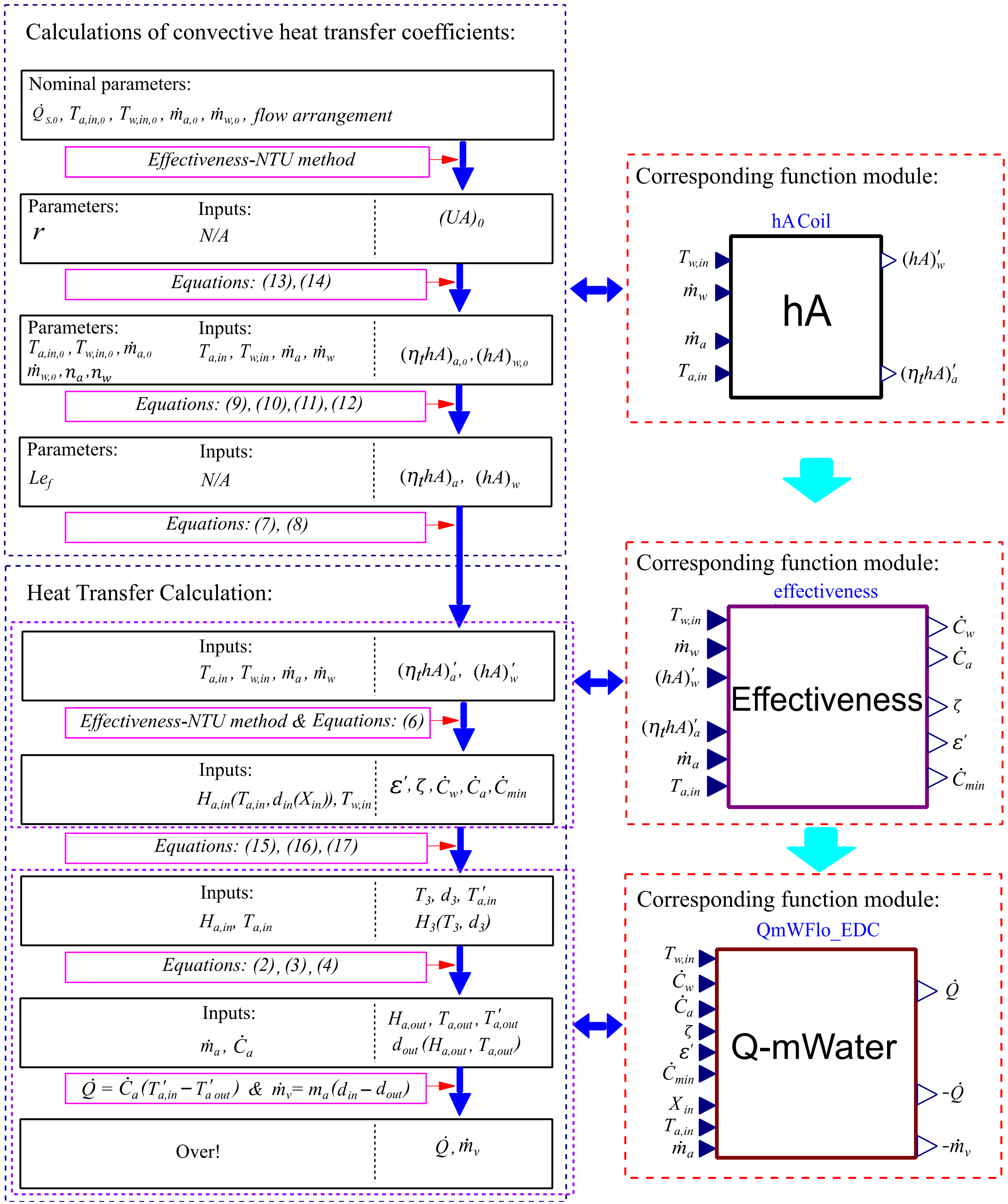

Fig. 2 Numerical scheme for implementing the new FTHE model

Fig. 2 shows the numerical scheme for the model implementations. The left side of the figure describes the procedures to calculate the convective heat transfer coefficients and simulate the heat transfer process, which is shown in section 2. The right side shows the corresponding function modules to be implemented in Modelica.

3.2. Modelica Model

Fig. 3 shows the implementations of the newly proposed FTHE model under wet-cooling condition in Modelica based on numerical scheme described in section 3.1. In Fig. 3, the fluid ports (inlets and outlets) connect the new FTHE model with an air-conditioning system. The *hA* module calculates the heat conductivity, and provides the results to the *Effectiveness* module to compute ζ and ε'. Then the *Q-m Water* module receives the values of ζ and ε', and calculates the heat transfer rate $\dot{Q}$ and mass flow rate of condensate water, $\dot{m}_v$, under non-nominal conditions. After that, the *Q-m Water* module provides $\dot{Q}$ to the *Static conservation equation 1* module (Water-side), and $-\dot{Q}$ and $-\dot{m}_v$ to the *Static conservation equation 2* module (Air-side). Since the air side is cooled and dehumidified, the values of $-\dot{Q}$ and $-\dot{m}_v$ are negative. It is noticed that these two *Static conservation equation* modules transport fluid between their two ports based on steady state simulation without storing or leaking mass or energy. In Fig. 3, *Mass fraction sensor* is used to measure the mass fraction of water vapor in air (X_{in}), which is utilized to calculate inlet humidity ratio d_{in}.

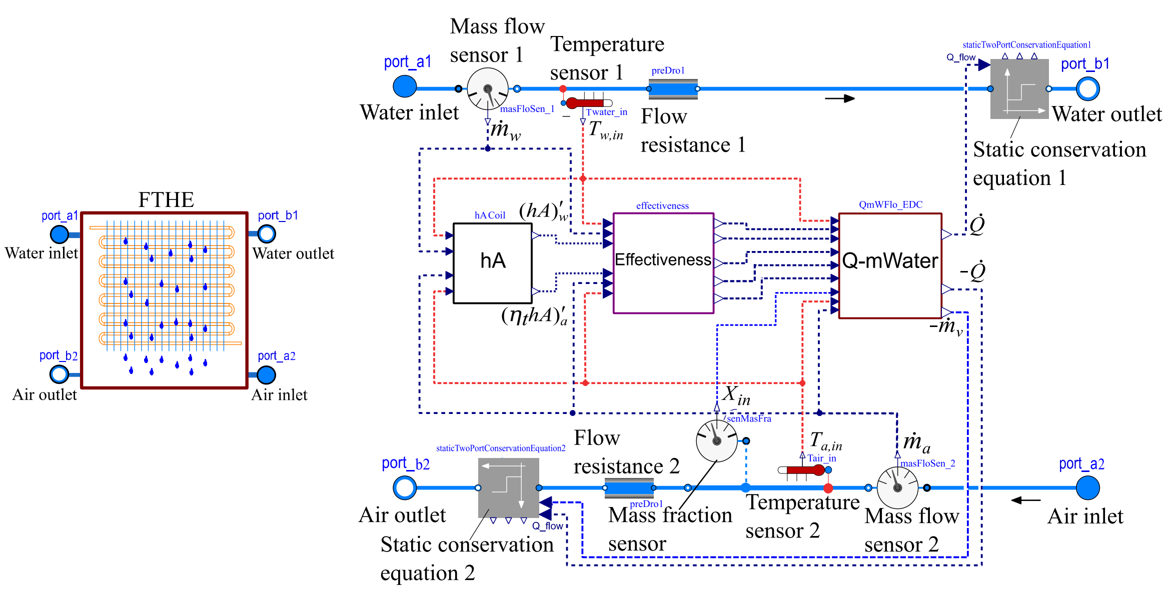

(a) Icon of FTHE model (b) Detailed construcion of FTHE model

Fig. 3. Modelica model of FTHE model under the wet-cooling condition

4. Experiment

4.1. Experiment Setup

To validate the new model, a prototype of water-to-air FTHE shown in Fig. 4 is used to conduct an experiment in a laboratory certified by the China National Accreditation Service for Conformity Assessment (CNAS). As shown Fig. 4, the water-to-air FTHE consists of a set of parallel round heat exchange tubes which are distributed uniformly within a block of parallel fins. A steel frame is used to fix heat exchange tubes and protect fins. The dispenser and collector tube are used to distribute and collect water from the heat exchange tubes. To ensure the accuracy of the results, Table 1 briefly summarizes the experimental conditions and relevant instruments.

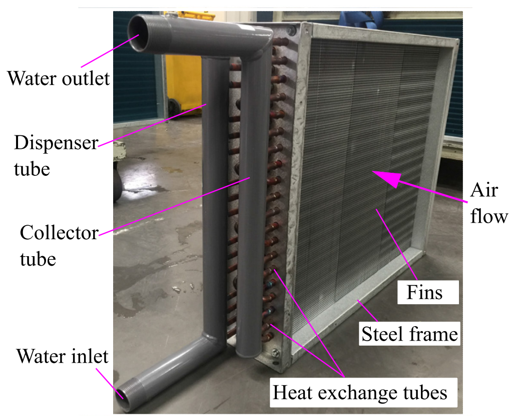

Fig. 4. Water-to-air FTHE used in the experiment

Table 1. The experimental conditions and instruments

Objects	Conditions	Instruments
Temperature	Measurement accuracy and control accuracy of temperatures are $\pm 0.05\ K$ and $\pm 0.2\ K$, respectively. Accuracy of thermocouple compensation wire is $\pm 0.1\ K$.	Platinum resistance thermometer, Pt100.
Water mass flow rate	Measurement tolerance of water mass flow rates is $\pm 1.0\%$.	Flow sensor, AXF040G

Air flow rate	Repeatability precision: the relative deviations between the three test results and their mean value are within $\pm 1.5\%$. Accuracy: the relative deviation between the tested FTHE and the standard prototype is within $\pm 2.0\%$.	Nozzles for air flow measurement (range: 0-1000 Pa). Pressure transmitter (range: 0-2.5 Mpa).
Heat transfer rate	Repeatability precision: the relative deviations between the three test results and their mean value are within $\pm 1.5\%$. Accuracy: the relative deviation between the tested FTHE and the standard prototype is within $\pm 2.0\%$.	N/A

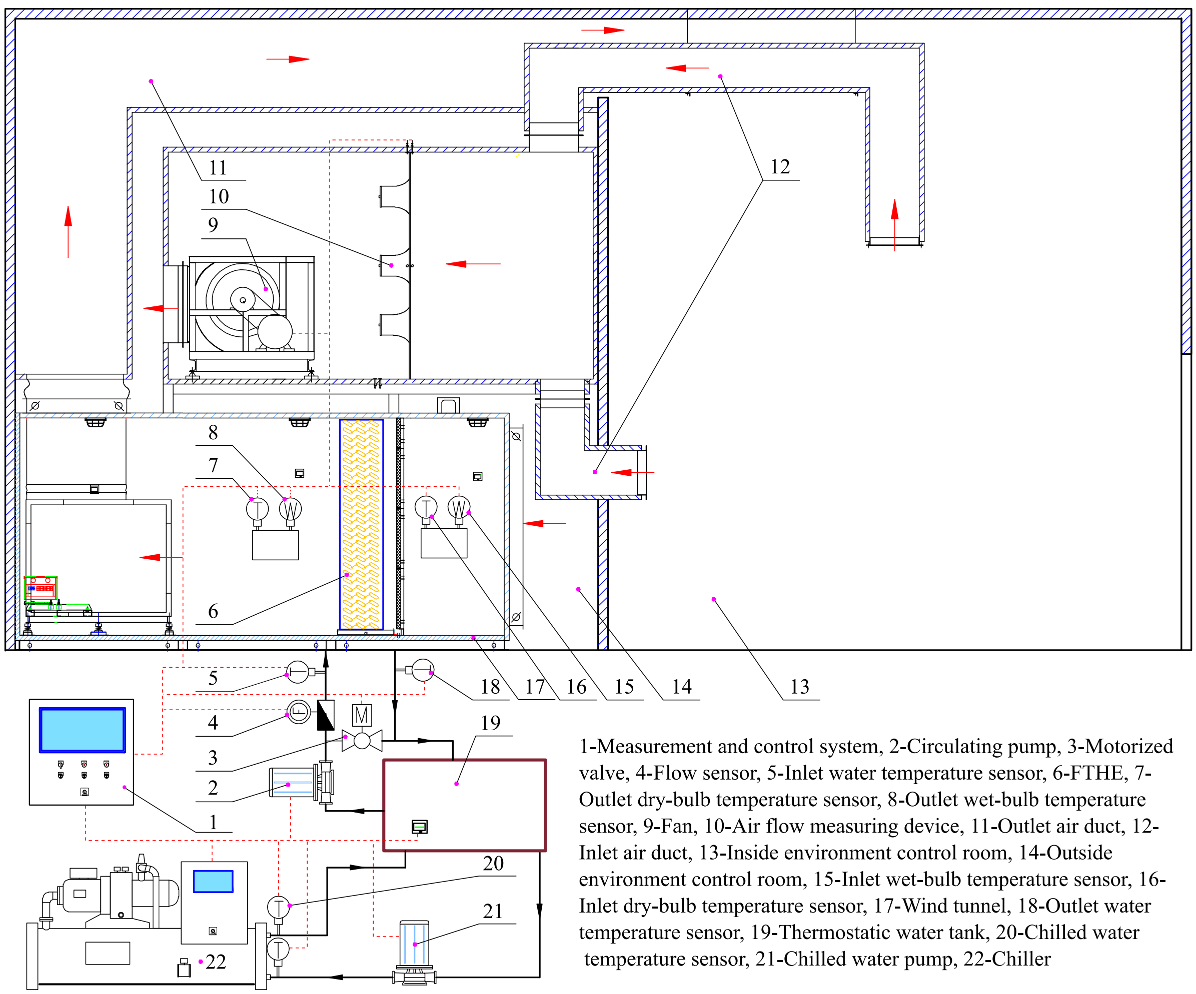

Fig. 5. Schematic of the experiment setup

Fig. 5 and Fig. 6 show the schematic of the experiment setup and main experimental facilities respectively. Main devices include control system, pumps, temperature, humidity and mass flow sensors, fan, nozzles air flow measurement, wind tunnel, thermostatic water tank, and chiller.

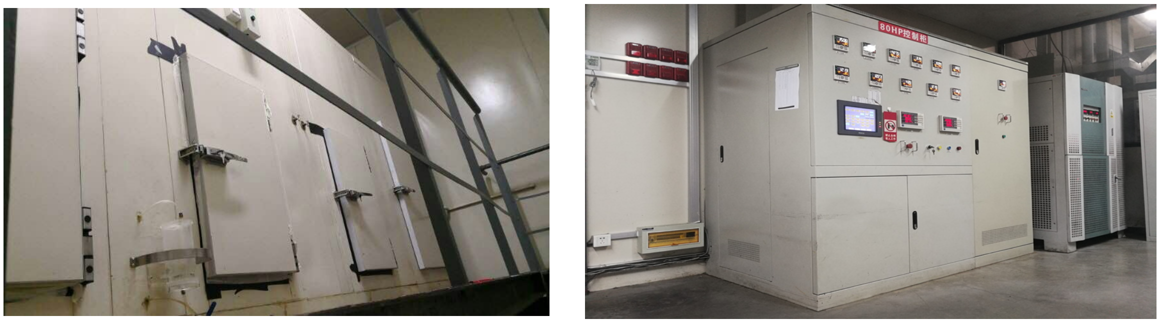

(a) Wind tunnel (b) Control system

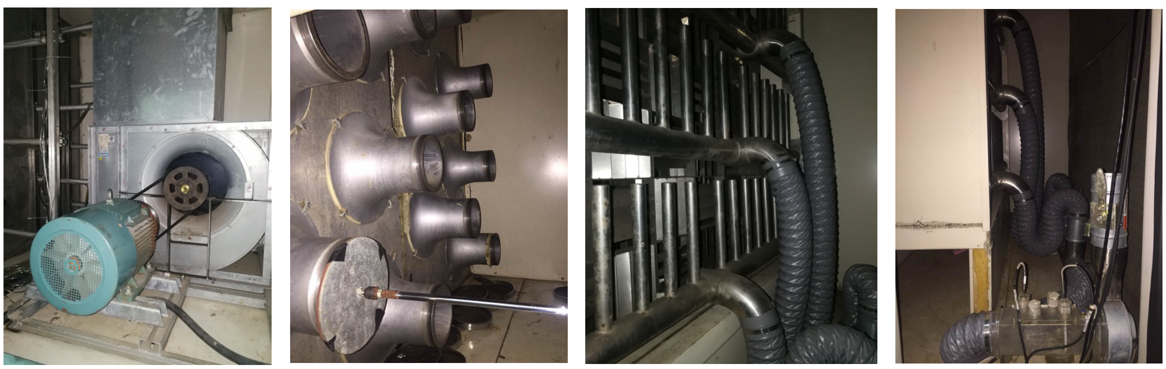

(c) Fan (d) Nozzles for air flow measurement (e) Air sampling apparatus (f) Measuring device of dry-bulb and wet-bulb temperatures

Fig. 6. Parts of experimental facilities

4.2. Experimental Data

Table 2 summaries the key parameters of the water-to-air FTHE experiments. Besides, the nominal data of this FTHE are: $\dot{Q}_0 = 86{,}040$ W, $\dot{Q}_{s0} = 35{,}562$ W, $\dot{m}_{a,0} = 2.004$ kg/s, $\dot{m}_{w,0} = 4.046$ kg/s, $T_{a,in,0} = 308.13$ K, $T_{w,in,0} = 280.13$ K, $X_{in,0} = 0.0209$, $T_{a,out,0} = 290.65$ K, and $T_{w,out,0} = 285.20$ K. Based on these nominal data, $(UA)_0 = 2{,}084.21$ W/K. These data are utilized to evaluate the performance of the newly proposed FTHE model. The main procedures and results are summarized in section 5.

Table 2. Experimental data of the water-to-air FTHE

Case	$\dot{m}_a$ (kg/s)	$\dot{m}_w$ (kg/s)	$T_{a,in}$ (K)	X_{in}	$T_{w,in}$ (K)	$T_{a,out}$ (K)	$T_{w,out}$ (K)	$\dot{Q}$ (W)
1	1.331	1.241	300.19	0.0109	280.13	286.46	285.12	26,535
2	1.478	1.341	300.03	0.0110	280.11	286.68	285.15	28,815

Case	$\dot{m}_a$ (kg/s)	$\dot{m}_w$ (kg/s)	$T_{a,in}$ (K)	X_{in}	$T_{w,in}$ (K)	$T_{a,out}$ (K)	$T_{w,out}$ (K)	$\dot{Q}$ (W)
3	1.774	1.522	300.07	0.0110	280.11	287.03	285.2	32,940
4	1.922	1.638	300.22	0.0109	280.12	287.36	285.16	35,115
5	2.070	1.688	300.26	0.0109	280.11	287.42	285.19	36,555
6	1.289	2.924	308.15	0.0209	280.12	288.89	285.16	61,960
7	1.432	3.180	308.14	0.0209	280.13	289.23	285.14	67,110
8	1.718	3.604	308.14	0.0209	280.18	289.92	285.23	76,515
9	1.861	3.927	308.13	0.0209	280.14	290.39	285.17	82,870

Uncertainty calculation is performed to analyze the measurement errors. In Table 2, the maximum measurement uncertainties of temperatures, water mass flow rates, air flow rates, water vapor mass fraction and heat transfer rates are within ± 0.20 K, ± 0.023 kg/s, ± 0.016 kg/s, ± 0.00023 and $\pm 3.46\%$, respectively.

5. Evaluation

To evaluate the newly developed FTHE model, we compare the computed results of the new model with an existing model, *WetCoilCounterFlow* (WCCF) from the Modelica Buildings Library [14, 65]. Both models are adopted to simulate the cases listed in Table 2. Based on experimental results, the relative deviations of the results obtained by the two models are compared. In addition, the computing speed is also discussed.

5.1. Reference Model: WCCF

The *WCCF* model is used to simulate counter flow heat exchangers with water vapor condensation, and the two-flow paths are discretized into N elements. Fig. 7 shows the top-level structure of the WCCF model in Modelica. In Fig. 7, the *HADryCoil* module has the similar function as the *hA* module in the new FTHE model. The difference between these two modules is that $(UA)_0$ needs to be given by users directly in *HADryCoil* module while in the *hA* module, it is not needed. The WCCF model has a *HexElementLatent* module which models the heat and mass exchanges between the discretized elements in both sides. In this module, the condensate water $\dot{m}_{v,i}$ is obtained by [66]:

$$\dot{m}_{v,i} = \frac{h_a A_i}{c_{p,a} Le_f} (X_{3,i} - X_i). \tag{22}$$

where A_i is the heat transfer area of each discretized element; $X_{3,i}$ and X_i are the water vapor mass fractions in the boundary layer and in the bulk of the air respectively in each discretized element; $Le_f = Le^{(1-b)}$, Le is Lewis number and b is a coefficient from the boundary layer analysis, typically $b = 1/3$ [66]; the subscript "i" represents the No. of microelement. The total condensate water $\dot{m}_v$ is the sum of all the $\dot{m}_{v,i}$. More details about the WCCF model are summarized in the Modelica Buildings Library [14, 65].

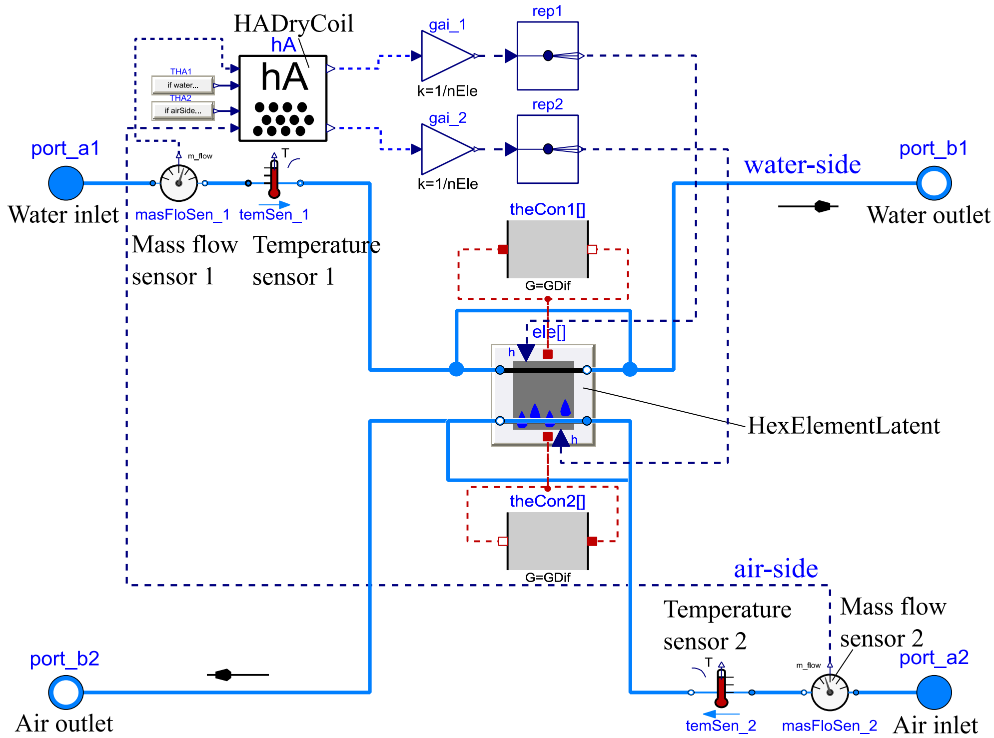

Fig. 7. Top-level structure of WCCF model in Modelica

5.2. Determination of Parameters

Before using these two models, the parameters need to be determined in advance. We use the method described in section 3.2 to set the parameters for the newly proposed FTHE model. The r and Le_f in the WCCF model are used to minimize the relative deviation of $\dot{Q}$ between the calculated and the measured values of heat transfer rate under nominal condition. Besides, N also needs to be determined by users in the WCCF model. The methods determining these parameters are described in the following paragraphs. For the remaining parameters, we obtain $(UA)_0 = 2{,}084.21$ W/K based on the nominal data and the values adopted in the FTHE model.

The first step is determining the values of r and Le_f. As mentioned above, the reasonable ranges for r and Le_f under nominal condition are $r \in [0.1, 0.5]$ and $Le_f \in [0.6, 1.3]$, respectively. We conduct the comparison of the simulation results with different combinations of r and Le_f with $N = 30$. Fig. 8 shows the relative deviations ($\dot{Q}$) of WCCF with various combinations of r and Le_f based on experimental data in nominal condition. The $relative\ deviation$ and $mean\ relative\ deviation$ are calculated by:

$$Relative\ deviation = \frac{|result\ of\ simulation - measurement|}{measurement} \times 100\% \quad (23)$$

$$Mean\ relative\ deviation = \frac{sum\ of\ mean\ Relative\ deviation\ \ at\ every\ case}{number\ of\ cases} \quad (24)$$

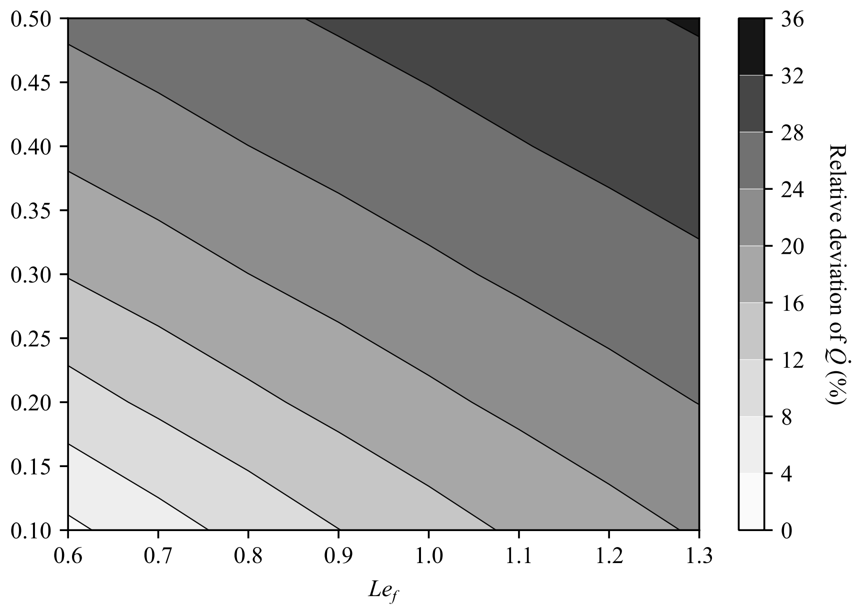

Fig. 8. Relative deviation of $\dot{Q}$ between WCCF under different various combinations of r and Le_f and experimental data

Fig. 8 shows that the relative deviation of $\dot{Q}$ increases when Le_f or r increases. As a result, the combination of $r = 0.1$ and $Le_f = 0.6$ is selected to minimize the relative deviation of $\dot{Q}$.

The next step is selecting appropriate value of N. We use Case 1 in Table 2 to identify the minimum N value, which could ensure the required accuracy. Fig. 9 shows the relative deviations of $\dot{Q}$ and computing time over different values of N (computer configuration: Inter® Xeon® CPU X-5675, 3.07GHz; 48GB memory). It clearly shows that when N is over 20, increasing N has neglectable impacts in decreasing relative deviation, but significantly increases computing time. The relationship between relative deviation of $\dot{Q}$ and computing time is correlated quantitatively as Eq. (25). It can be found that the minimum value of the relative deviation is 11.461%. Considering reasonable accuracy and computing time cost, it is acceptable that the relative deviation of $\dot{Q}$ deviates from its minimum value within 10%. Thus, we set $N = 32$ in WCCF model and the corresponding relative deviation of $\dot{Q}$ is 12.57% which is only slightly larger than the minimum value (11.46%) obtained with $N \to \infty$.

$$Relative\ deviation\ of\ \dot{Q} = \left(\frac{34.123}{computing\ time} + 11.461\right)\% \tag{25}$$

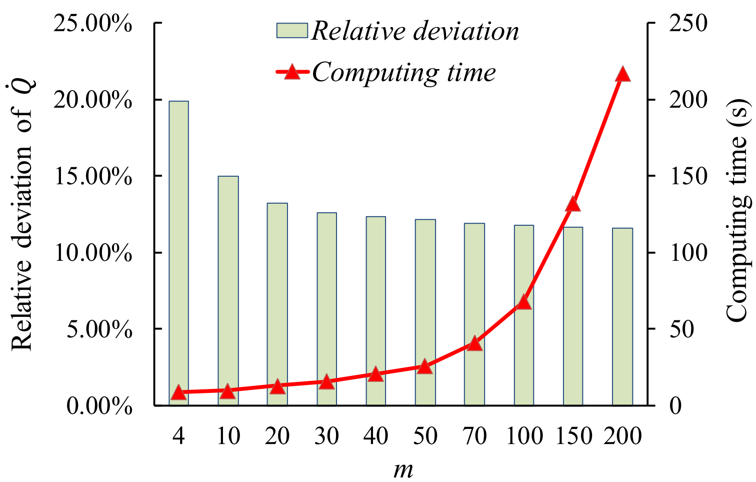

Fig. 9. Relative deviation of $\dot{Q}$ and computing time over different m under Case 1 (WCCF model)

Table 3 summaries all the parameters in the newly developed FTHE model and existing WCCF model. The performances of the two models were evaluated by comparing with the experimental data in Table 2. In each case, the iterations continue until the relative deviation is lower than 1E-4.

Table 3. Parameters setting for evaluation simulations

	$\dot{m}_{a,0}$ (kg/s)	$\dot{m}_{w,0}$ (kg/s)	$T_{a,in,0}$ (K)	$T_{w,in,0}$ (K)	$\dot{Q}_{s,0}$ (W)	$(UA)_0$ (W/K)	n_a	n_w	r	Le_f	N
FTHE	2.004	4.046	308.13	280.13	35,562	N/A	0.65	0.85	0.209	0.6	N/A
WCCF	2.004	4.046	308.13	280.13	N/A	2,084.21	0.65	0.85	0.100	0.6	32

5.3. Comparison of Accuracy

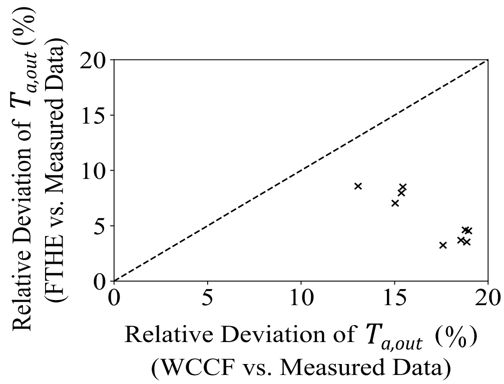

(a) $T_{a,out}$

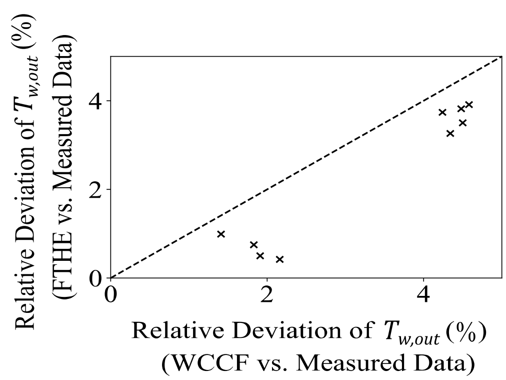

(b) $T_{w,out}$

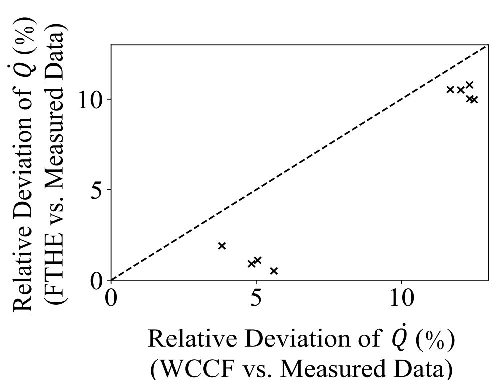

(c) $\dot{Q}$

Fig.10. Comparison of the new FTHE model and WCCF model with experimental data

The relative deviations of $T_{a,out}$, $T_{w,out}$, and $\dot{Q}$ obtained by model predictions and experimental data are shown in Fig.10. Here, the Celsius scale was used to calculate the relative deviation of temperature. Therefore, when

Eq. (23) is adopted to calculate the relative deviation of temperatures, its denominator is changed from "$measurement$" to "$measurement - 273.15$". In Fig.10, the new FTHE model has a better performance in prediction accuracy. Fig.10(a) shows that the m$ean\ relative\ deviation$ of $T_{a,out}$ is 5.20% for the new FTHE model and 16.85% for the existing WCCF model respectively. The maximum $relative\ deviation$ of $T_{a,out}$ is 6.15% for the new FTHE model and 18.95% for the WCCF model. Fig.10(b) illustrates that the m$ean\ relative\ deviation$ of $T_{w,out}$ is 2.32% for the new FTHE model and 3.27% for the WCCF model while the maximum $relative\ deviation$ of $T_{w,out}$ is 3.91% for the new FTHE model and 4.58% for the WCCF model. Fig.10(c) shows the m$ean\ relative\ deviation$ of $\dot{Q}$ is 6.52% for the new FTHE model and 8.92% for the WCCF model, and the maximum $relative\ deviation$ of $\dot{Q}$ is 10.79% for the new FTHE model and 12.51% for the WCCF model.

The new FTHE model has a better performance because it uses an indirect solution to determine the $\dot{m}_v$. This indirect solution avoids the inconvenience and errors caused by directly solving the condensate water and latent heat equations. On the contrary, the WCCF model uses a direct approach to derive the $\dot{m}_v$ as Eq. (22). In Eq. (22), the derivation of $X_{3,i}$ was based on an approximation correlating the partial pressure of saturation water vapor and saturation $T_{3,i}$ [14]. At the same time, X_i in the bulk of air is replaced by the outlet water vapor mass fraction $X_{i,out}$ to conduct the approximate calculation. These approximations inevitably lead to some errors. Moreover, discrepancies exist in the calculations of $T_{3,i}$ and $X_{i,out}$. The heat transfer and mass transfer are calculated simultaneously in the WCCF model. The errors of the mass transfer calculation inevitably influence the sensible heat transfer rate. Based on the discussions, it can be explained that the relative deviations of $T_{a,out}$, $T_{w,out}$ and $\dot{Q}$ in the new FTHE model are smaller than those in the WCCF model.

5.4. Comparison of Computing Speed

Fig.11 compares the computing time of the newly developed FTHE and existing WCCF models. In this figure, the convergence procedure of $T_{a,out}$ corresponds to the case 1 in Table 2. It can be seen that after 15 s (physical time), the convergences of $T_{a,out}$ of the two models are obtained perfectly. The new FTHE model takes about 0.01 s CPU time to complete the simulation of a 15 s long heat transfer process, while the WCCF model needs about 10.47 s. Thus, the new FTHE model is about 1047 times faster than the WCCF model, due to the fact that the WCCF model needs to solve additional 205 differential-algebraic equations for each discretized element. Totally, the WCCF model needs to solve about 6,776 equations for 32 elements, while the new FTHE model only needs to solve about 272 equations.

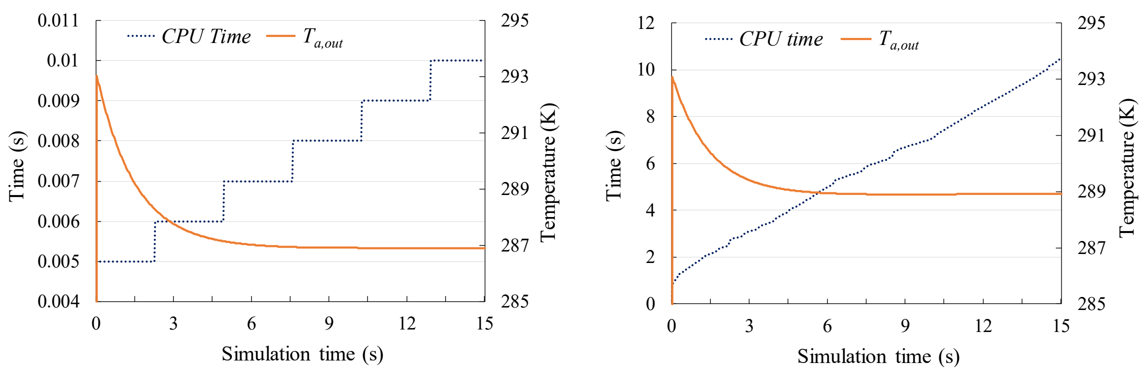

(a) FTHE model (b) WCCF model

Fig.11. Comparison of computing time of the new FTHE and WCCF models

6 Conclusion

This paper proposes a new water-to-air FTHE mathematical model for wet cooling conditions using wet-dry transformation method. The model only requires nominal data as inputs. The new model is implemented using Modelica. Experimental measurement is conducted for the model validation. The new FTHE model is then compared with an existing model and experimental data. The results show that the relative deviations of outlet temperatures between the modeled results and experimental data are within 7% for the new model and 19% for the existing model, respectively. The relative deviations of heat transfer rate are lower than 11% for the new model and 13% for the existing model. Meanwhile, the new model is about 1047 times faster than the existing model.

Acknowledgement

This work was supported by the National Science Foundation of USA [No. IIS-1802017]. This work was also supported by the key project fund for the collaborative innovation of the universities from the Bureau of Education of Guangzhou City in China [No.1201610004] and the special fund for energy saving research from the Guangzhou Housing and Urban-Rural Construction Committee in China [No. J-2016-11].

References

[1] C.R. Ruivo, F. Dominguez-Muñoz, J.J. Costa, Simplified model of finned-tube heat exchangers based on the effectiveness method and calibrated with manufacturer and experimental data, Applied Thermal Engineering, 111 (2017) 340-352.

[2] W. Pirompugd, S. Wongwises, Actual dry-bulb temperature and equivalent dry-bulb temperature methods for wavy fin-and-tube heat exchangers with dehumidification, International Journal of Heat and Mass Transfer, 106 (2017) 675-685.

[3] M.L. Ni, Guangyuan; Yang, Weibo; Ma Rongsheng and Xie, Zhixiang, Comparison and analysis of thermal calculation methods for surface air coolers, HV & AC, 38 (2008) 75-78. (in Chinese)

[4] F.Y. Ling, Chunjie, Simplified heat exchanger model of fan coil in wet cooling conditons, HV&AC, 42 (2012) 105-109. (in Chinese)

[5] L. Xia, M.Y. Chan, S.M. Deng, X.G. Xu, Analytical solutions for evaluating the thermal performances of wet air cooling coils under both unit and non-unit Lewis Factors, Energy Conversion and Management, 51 (2010) 2079-2086.

[6] V.S.K.V. Harish, A. Kumar, Reduced order modeling and parameter identification of a building energy system model through an optimization routine, Applied Energy, 162 (2016) 1010-1023.

[7] M. Wetter, Simulation model finned water-air-coil withoutcondensation, in, Ernest Orlando Lawrence Berkeley National Laboratory, Berkeley, CA (US), 1999.

[8] M.K. Mansour, M. Hassab, Novel approach of thermal modeling of partially dry–wet chilled water cooling coil under unit and nonunit Lewis number conditions, Numerical Heat Transfer, Part B: Fundamentals, 70 (2016) 164-181.

[9] M.K. Mansour, Practical effectiveness-NTU model for cooling and dehumidifying coil with non-unit Lewis Factor, Applied Thermal Engineering, 100 (2016) 1111-1118.

[10] W. Pirompugd, S. Wongwises, C.-C. Wang, A tube-by-tube reduction method for simultaneous heat and mass transfer characteristics for plain fin-and-tube heat exchangers in dehumidifying conditions, Heat and mass transfer, 41 (2005) 756-765.

[11] A. Vardhan, P.L. Dhar, A new procedure for performance prediction of air conditioning coils, International Journal of Refrigeration, 21 (1998) 77-83.

[12] W. Pirompugd, C.-C. Wang, S. Wongwises, A fully wet and fully dry tiny circular fin method for heat and mass transfer characteristics for plain fin-and-tube heat exchangers under dehumidifying conditions, Journal of Heat Transfer, 129 (2007) 1256-1267.

[13] W. Pirompugd, C.C. Wang, S. Wongwises, Finite circular fin method for heat and mass transfer characteristics for plain fin-and-tube heat exchangers under fully and partially wet surface conditions, International Journal of Heat & Mass Transfer, 50 (2007) 552-565.

[14] M. Wetter, W. Zuo, T.S. Nouidui, X. Pang, Modelica buildings library, Journal of Building Performance Simulation, 7 (2014) 253-270.

[15] F.E. Romie, Transient Response of the Counterflow Heat Exchanger, Journal of Heat Transfer, 106 (1984) 620-626.

[16] C.C. Lakshmanan, O.E. Potter, Dynamic simulation of a countercurrent heat exchanger modelling-start-up and frequency response, International Communications in Heat & Mass Transfer, 21 (1994) 421-434.

[17] XiaotangZhou, J. Braun, A Simplified Dynamic Model for Chilled-Water Cooling and Dehumidifying Coils—Part 1: Development (RP-1194), Hvac & R Research, 13 (2007) 785-804.

[18] S.J. Cao, X.R. Kong, Y. Deng, W. Zhang, L. Yang, Z.P. Ye, Investigation on thermal performance of steel heat exchanger for ground source heat pump systems using full-scale experiments and numerical simulations, Applied Thermal Engineering, 115 (2017) 91-98.

[19] S. Bielski, L. Malinowski, An analytical method for determining transient temperature field in a parallel-flow three-fluid heat exchanger, International Communications in Heat and Mass Transfer, 32 (2005) 1034-1044.

[20] G. Bandyopadhyay, W. Gosnold, M. Mann, Analytical and semi-analytical solutions for short-time transient response of ground heat exchangers, Energy and Buildings, 40 (2008) 1816-1824.

[21] J. Yin, M.K. Jensen, Analytic model for transient heat exchanger response, International Journal of Heat & Mass Transfer, 46 (2003) 3255-3264.

[22] M. Spiga, G. Spiga, Transient Temperature Fields in Crossflow Heat Exchangers With Finite Wall Capacitance, Journal of Heat Transfer, 110 (1988) 49-53.

[23] J.L. Threlkeld, Thermal environmental engineering, Prentice Hall, 1970.

[24] A.L. London, Compact Heat Exchangers: A Festschrift for AL London, CRC Press, 1990.
[25] R.K. Shah, D.P. Sekulic, Fundamentals of heat exchanger design, John Wiley & Sons, 2003.
[26] J. Wang, E. Hihara, Prediction of air coil performance under partially wet and totally wet cooling conditions using equivalent dry-bulb temperature method, International Journal of Refrigeration, 26 (2003) 293-301.
[27] J. Wang, Heat transfer study of surface air coolers (1): Wet dry transformation method for thermodynamic calculation of the wet cooling condition [J], HV & AC, 4 (2000). (in Chinese)
[28] W. Pirompugd, C.C. Wang, S. Wongwises, The New Mathematical Models for Plain Fin-and-Tube Heat Exchangers With Dehumidification, Journal of Heat Transfer, 27 (2015).
[29] DoE, EnergyPlus Engineering Reference. US Department of Energy, in, 2016.
[30] S. Klein, W. Beckman, J. Mitchell, J. Duffie, N. Duffie, T. Freeman, J. Mitchell, J. Braun, B. Evans, J. Kummer, et al, TRNSYS 17. A TRaNsient SYstem Simulation Program; Mathematical Reference, Solar Energy Laboratory, University of Wisconsin-Madison: Madison, WI, USA, 4 (2014).
[31] S. Klein, W. Beckman, J. Mitchell, J. Duffie, N. Duffie, T. Freeman, J. Mitchell, J. Braun, B. Evans, J. Kummer, et al, TRNSYS 18. A TRaNsient SYstem Simulation Program; Standard Component Library Overview, Solar Energy Laboratory, University of Wisconsin-Madison: Madison, WI, USA, 3 (2017).
[32] J. Thornton, D. Bradley, T. McDowell, N. Blair, M. Duffy, N. LaHam, A. Naik, et al, TESSLibs 17 HVAC Library Mathematical Reference, Thermal Energy System Specialists, Madison, Wisconsin, (2014).
[33] Y. Ye, M. Huang, J. Mo, S. Dai, State-space model for transient behavior of water-to-air surface heat exchanger, International Journal of Heat & Mass Transfer, 64 (2013) 173-192.
[34] Ö.E. Ataer, An approximate method for transient behavior of finned-tube cross-flow heat exchangers, International Journal of Refrigeration, 27 (2004) 529-539.
[35] G.Y. Jin, W.J. Cai, Y.W. Wang, Y. Yao, A simple dynamic model of cooling coil unit, Energy Conversion & Management, 47 (2006) 2659-2672.
[36] X.R. Kong, Y. Deng, L. Li, W.S. Gong, S.J. Cao, Experimental and numerical study on thermal performance of ground source heat pump with a set of designed buried pipes, Applied Thermal Engineering, 114 (2017) 110-117.
[37] V.P. Kabashnikov, L.N. Danilevskii, V.P. Nekrasov, I.P. Vityaz, Analytical and numerical investigation of the characteristics of a soil heat exchanger for ventilation systems, International Journal of Heat and Mass Transfer, 45 (2002) 2407-2418.
[38] R. Chengqin, Y. Hongxing, An analytical model for the heat and mass transfer processes in indirect evaporative cooling with parallel/counter flow configurations, International Journal of Heat and Mass Transfer, 49 (2006) 617-627.
[39] Z. Lian, Fundamentals & Equipment of Heat & Mass Transfer, 3 ed., China Building Industry Press, Beijing,China, 2011. (in Chinese)
[40] J.C. Kloppers, D.G. Kröger, The Lewis factor and its influence on the performance prediction of wet-cooling towers, International Journal of Thermal Sciences, 44 (2005) 879-884.
[41] S. Tan, The Application for Design Optimization of the Plate-Fin Heat Exchanger Based on Genetic Algorithm, in, Vol. Master's thesis, Anhui University of Technology Ma anshan, China, 2013. (in Chinese)
[42] C.H. Li Conglai, Shu Chaohui and Lu Hongliang, , The analysis and research of calculation method for the wet air parameter The Proceedings of 2008 National HVAC&R Academic Conference, (2008). (in Chinese)
[43] A. Handbook, Fundamentals, SI ed, American Society of Heating, Refrigerating and Air Conditioning Engineers: Atlanta, GA, USA, (2009).
[44] Y. Lu, Practical heating and air conditioning design manual, China Building Industry Press, Beijing, (2008). (in Chinese)
[45] W.D. Han, Guoliang; Hu, Haitao; Zhuang, Dawei, A Numerical Study of Lewis Factor for Fin-and-tube Heat Exchangers under Dehumidifying Conditions, Journal of Refrigeration, 33(6) (2012) 46-51.
[46] L. Xia, M. Chan, S. Deng, X. Xu, Analytical solutions for evaluating the thermal performances of wet air cooling coils under both unit and non-unit Lewis Factors, Energy Conversion and Management, 51 (2010) 2079-2086.
[47] H.L. Kang, Bin;Li Huizhen;Xin Rongchang;Tao,Wenquan, Experimental Study on Heat Transfer and Pressure Drop for Plane Fin-and-Tube Heat Exchanger, Journal of Xi'an Jiaotong University, 28 (1994) 91-98. (in Chinese)
[48] C.-C. Wang, W.-H. Tao, C.-J. Chang, An investigation of the airside performance of the slit fin-and-tube heat exchangers, International Journal of Refrigeration, 22 (1999) 595-603.

[49] C.-C. Wang, C.-J. Lee, C.-T. Chang, Y.-J. Chang, Some aspects of plate fin-and-tube heat exchangers: with and without louvers, Journal of Enhanced Heat Transfer, 6 (1999).
[50] W.W. Liu jian, Ding Guoliang and Zhang Chunlu, Development of Experimental Research on Heat Transfer and Friction Characteristics of Fin-and-tube Heat Exchanger —Correlation, Journal of Refrigeration, (2003) 21-27. (in Chinese)
[51] A. Kumar, J.B. Joshi, A.K. Nayak, P.K. Vijayan, A review on the thermal hydraulic characteristics of the air-cooled heat exchangers in forced convection, Sadhana, 40 (2015) 673-755.
[52] T.A. Tahseen, M. Ishak, M.M. Rahman, An overview on thermal and fluid flow characteristics in a plain plate finned and un-finned tube banks heat exchanger, Renewable and Sustainable Energy Reviews, 43 (2015) 363-380.
[53] Y. Jin, Z.-Q. Yu, G.-H. Tang, Y.-L. He, W.-Q. Tao, Parametric study and multiple correlations of an H-type finned tube bank in a fully developed region, Numerical Heat Transfer, Part A: Applications, 70 (2016) 64-78.
[54] A.A. Bhuiyan, A.K.M.S. Islam, Thermal and hydraulic performance of finned-tube heat exchangers under different flow ranges: A review on modeling and experiment, International Journal of Heat and Mass Transfer, 101 (2016) 38-59.
[55] T.L. Bergman, F.P. Incropera, Fundamentals of heat and mass transfer, John Wiley & Sons, 2011.
[56] S.E. Mattsson, H. Elmqvist, Modelica - An International Effort to Design the Next Generation Modeling Language, 30 (1997) 151-155.
[57] W. Tian, T.A. Sevilla, W. Zuo, M.D. Sohn, Coupling fast fluid dynamics and multizone airflow models in Modelica Buildings library to simulate the dynamics of HVAC systems, Building & Environment, 122 (2017).
[58] W. Zuo, M. Wetter, W. Tian, D. Li, M. Jin, Q. Chen, Coupling indoor airflow, HVAC, control and building envelope heat transfer in the Modelica Buildings library, Journal of Building Performance Simulation, 9 (2016) 366-381.
[59] S. Huang, A.C.L. Malara, W. Zuo, M.D. Sohn, A Bayesian network model for the optimization of a chiller plant's condenser water set point, Journal of Building Performance Simulation, 11 (2016) 1-12.
[60] S. Huang, W. Zuo, M.D. Sohn, Amelioration of the cooling load based chiller sequencing control, Applied Energy, 168 (2016) 204-215.
[61] S. Huang, W. Zuo, M.D. Sohn, Improved cooling tower control of legacy chiller plants by optimizing the condenser water set point, Building & Environment, 111 (2017) 33-46.
[62] R. Miranda, S. Huang, G. Barrios, D. Li, W. Zuo, Energy Efficient Design for Hotels in the Tropical Climate using Modelica, in: The International Modelica Conference, 2015, pp. 71-78.
[63] G. Zhou, Y. Ye, W. Zuo, X. Zhou, Modelling water-cooled air coolers under wet-cooing conditions, in: Proceedings of 2017 National Academic Conference on HVAC Simulation, Guangzhou, China, 2017. (in Chinese)
[64] G. Zhou, Y. Ye, W. Zuo, X. Zhou, Modelling air-to-air plate-fin heat exchanger without condensation, in: Proceedings of the 4th International Conference On Building Energy & Environment 2018 Conference On Building Energy & Environment - COBEE2018, Melbourne, Australia, 2018.
[65] M. Wetter, M. Bonvini, T.S. Nouidui, W. Zuo, Modelica Buildings library 2.0, in: Proc. of The 14th International Conference of the International Building Performance Simulation Association (Building Simulation 2015), Hyderabad, India, 2015.
[66] M. Wetter, Modelica library for building heating, ventilation and air-conditioning systems, Lawrence Berkeley National Laboratory, (2010).

Appendix A. Detailed mathematical derivation of the new FTHE model

1. Derivation of Contact Factor ζ

Under the wet-cooling condition, the air losses the heat $d\dot{Q}$ within the dA can also be calculated by:

$$d\dot{Q} = -\dot{m}_a dH. \tag{A.1}$$

According to Eq. (5) in the main body of the paper and Eq. (A.1), we can get:

$$\frac{dH}{H - H_3} = -\frac{\eta_t h_a dA}{\dot{C}_a \, Le_f}, \tag{A.2}$$

where $\dot{C}_a$ is the heat capacity rate of air flow and $\dot{C} = \dot{m}c_p$. In Eq. (A.2), H_3 is the average enthalpy of the saturated air near the tube wall and is a constant. So, the integral of Eq. (A.2) in the whole computational domain can be expressed as:

$$\int_{H_{a,in}}^{H_{a,out}} \frac{d(H - H_3)}{H - H_3} = \int_0^A -\frac{\eta_t h_a dA}{\dot{C}_a \, Le_f}, \tag{A.3}$$

where A is the whole heat transfer area. Eq. (A.3) is calculated as

$$\frac{H_{a,in} - H_{a,out}}{H_{a,in} - H_3} = 1 - exp\left[-\frac{(\eta_t hA)_a}{\dot{C}_a \, Le_f}\right]. \tag{A.4}$$

According Eq. (1) in the main body of the paper and Eq. (A.4), ζ can be calculated by:

$$\zeta = 1 - exp\left[-\frac{(\eta_t hA)_a}{\dot{C}_a \, Le_f}\right]. \tag{A.5}$$

Under the equivalent dry-cooling condition, $d\dot{Q}'$ is:

$$d\dot{Q}' = \eta_t h_a'(T' - T_3)dA, \tag{A.6}$$

where h_a' is the convective heat transfer coefficient under the equivalent dry-cooling condition. At the same time, the air losses the heat $d\dot{Q}'$ within the dA:

$$d\dot{Q}' = -\dot{m}_a' c_{p,a} dT'. \tag{A.7}$$

Based on Eq. (A.6) and Eq. (A.7), the equation is rewritten as:

$$\frac{dT'}{T' - T_3} = -\frac{\eta_t h_a' dA}{\dot{C}_a'}. \tag{A.8}$$

In, Eq. (A.8), T_3 is the average temperature of the saturated air near the tube wall and constant on the surface of the tube. So, the Eq. (A.8) in the whole computational domain can be expressed as:

$$\int_{T_{a,in}'}^{T_{a,out}'} \frac{d(T' - T_3)}{T' - T_3} = \int_0^A -\frac{\eta_t h_a' dA}{\dot{C}_a}. \tag{A.9}$$

Then

$$\frac{T_{a,in}' - T_{a,out}'}{T_{a,in}' - T_3} = 1 - exp\left[-\frac{(\eta_t hA)_a'}{\dot{C}_a}\right]. \tag{A.10}$$

According to Eq. (2) in the main body of the paper and Eq. (A.10):

$$\zeta = 1 - exp\left[-\frac{(\eta_t hA)'_a}{\dot{C}_a}\right]. \tag{A.11}$$

Based on Eq. (A.5) and Eq. (A.11), we can get the Eq. (6) shown in the main body.

2. Calculation of $(UA)_0$

In the assumed independent sensible heat transfer process, the heat flow rate is $\dot{Q}_{s,0}$, the overall heat transfer coefficient is U_0 and inlet temperatures and mass flow rates are $\dot{m}_{a,0}$, $\dot{m}_{w,0}$, $T_{a,in,0}$ and $T_{w,in,0}$. Then, the heat transfer effectiveness can be calculated by:

$$\varepsilon_0 = \frac{\dot{Q}_{s,0}}{\dot{Q}_{max,0}}, \tag{A.12}$$

where $\dot{Q}_{max,0}$ is the possibly maximum heat transfer rate:

$$\dot{Q}_{max,0} = \dot{C}_{min,0}\left|T_{w,in,0} - T_{a,in,0}\right|, \tag{A.13}$$

and

$$\dot{C}_{min,0} = min(\dot{C}_{a,0}, \dot{C}_{w,0}), \tag{A.14}$$

where, $\dot{C}_{a,0}$ and $\dot{C}_{w,0}$ are the heat capacity rate of the air flow and water flow under nominal condition. The capacity rate ratio $R_{C,0}$ is defined as:

$$R_{C,0} = \frac{\dot{C}_{min,0}}{\dot{C}_{max,0}}, \tag{A.15}$$

where,

$$\dot{C}_{max,0} = max(\dot{C}_{a,0}, \dot{C}_{w,0}). \tag{A.16}$$

The number of heat transfer units NTU_0 is:

$$NTU_0 = f(\varepsilon_0, R_{C,0}, flow\ arrangement), \tag{A.17}$$

where, $flow\ arrangement$ is a parameter in this new FTHE model. It is associated with the structure of heat exchanger. Specific formulas of Eq. (A.17) for different heat exchanger flow arrangements are listed in Table A.1.

Table A.1. Equations of ε and NTU for different heat exchanger flow arrangements [29]

Flow arrangement	$\varepsilon = f(NTU, R_C, flow\ arrangement)$	$NTU = f(\varepsilon, R_C, flow\ arrangement)$
counter flow heat exchanger	$\varepsilon = \frac{1 - exp[-NTU(1 - R_C)]}{1 - R_C exp[-NTU(1 - R_C)]}$	$NTU(R_C \neq 1) = \frac{1}{R_C - 1}\ln(\frac{1 - \varepsilon}{1 - \varepsilon R_C})$

		$NTU(R_C = 1) = \frac{\varepsilon}{1-\varepsilon}$
parallel flow heat exchanger	$\varepsilon = \frac{1 - exp[-NTU(1+R_C)]}{1+R_C}$	$NTU = \frac{\ln(-\varepsilon - \varepsilon R_C + 1)}{R_C + 1}$
cross flow heat exchanger with two streams unmixed	$\varepsilon = 1 - exp\left\{\frac{NTU^{0.22}}{R_C}[exp(-R_C NTU^{0.78}) - 1]\right\}$	$NTU = f(\varepsilon, NTU, R_C)$
cross flow heat exchanger with two streams mixed	$\varepsilon = \left[\frac{1}{1-exp(-NTU)} + \frac{R_C}{1-exp(-R_C NTU)} - \frac{1}{NTU}\right]^{-1}$	$NTU = f(\varepsilon, NTU, R_C)$
cross flow heat exchanger with the stream with the higher capacity mixed and the stream with the lower capacity unmixed	$\varepsilon = \frac{1}{R_C}\{1 - exp[R_C(exp(-NTU) - 1)]\}$	$NTU = -\ln\left[\frac{\ln(1-\varepsilon R_C)}{R_C} + 1\right]$
cross flow heat exchanger with the stream with higher capacity unmixed and the stream with lower capacity mixed	$\varepsilon = 1 - exp\left\{-\frac{1}{R_C}[1 - exp(-R_C NTU)]\right\}$	$NTU = \frac{-\ln[R_C \ln(1-\varepsilon) + 1]}{R_C}$

$(UA)_0$ is calculated by:

$$(UA)_0 = \dot{C}_{min,0} NTU_0. \tag{A.18}$$

3. Calculation of ε' and $T'_{a,in}$

The overall heat transfer coefficient $(UA)'$ under equivalent dry-cooling condition is calculated by [41]:

$$(UA)' = \left[\frac{1}{(hA)'_w} + \frac{1}{(\eta_t hA)'_a}\right]^{-1}. \tag{A.19}$$

The number of exchanger heat transfer units NTU' is:

$$NTU' = \frac{(UA)'}{\dot{C}'_{min}} = \frac{(UA)'}{\dot{C}_{min}}, \tag{A.20}$$

where

$$\dot{C}'_{min} = \dot{C}_{min} = min(\dot{C}_a, \dot{C}_w), \tag{A.21}$$

where $\dot{C}_w$ is the heat capacity rate of water flow. Then the heat transfer effectiveness ε' is calculated by:

$$\varepsilon' = f(NTU', R'_C, flow\ arrangement), \tag{A.22}$$

where

$$R'_C = \frac{\dot{C}'_{min}}{\dot{C}'_{max}} = \frac{\dot{C}_{min}}{\dot{C}_{max}}. \tag{A.23}$$

In Eq. (A.23),

$$\dot{C}'_{max} = \dot{C}_{max} = max\left(\dot{C}_a, \dot{C}_w\right). \tag{A.24}$$

The heat transfer effectiveness, ε', is defined as the actual heat transfer $\dot{Q}'$ divided by the maximum possibly heat transfer $\dot{Q}'_{max}$:

$$\varepsilon' = \frac{\dot{Q}'}{\dot{Q}'_{max}} \tag{A.25}$$

The actual heat transfer rate $\dot{Q}'$ is:

$$\dot{Q}' = \dot{C}'_a\left(T'_{a,in} - T'_{a,out}\right) = \dot{C}_a\left(T'_{a,in} - T'_{a,out}\right). \tag{A.26}$$

The maximum possibly heat transfer rate $\dot{Q}'_{max}$ can be calculated by:

$$\dot{Q}'_{max} = \dot{C}'_{min}\left(T'_{a,in} - T'_{w,in}\right) = \dot{C}_{min}\left(T'_{a,in} - T_{w,in}\right). \tag{A.27}$$

Substituting Eq. (A.26) and Eq. (A.27) into Eq. (A.25):

$$\varepsilon' = \frac{\dot{C}_a(T'_{a,in} - T'_{a,out})}{\dot{C}_{min}\left(T'_{a,in} - T_{w,in}\right)}. \tag{A.28}$$

According to Eq. (2) in the main body of the paper, $T'_{a,out}$ can be calculated by:

$$T'_{a,out} = T'_{a,in} - \zeta\left(T'_{a,in} - T_3\right). \tag{A.29}$$

Then Eq. (A.29) is substituted into Eq. (A.28), we can get $\mathrm{T}'_{\mathrm{a,in}}$ as the Eq. (15) shown in the main body.